Impact of Electric Vehicles on Power Quality in Central Charging Infrastructures

Friedemann Möller, Sascha Müller, Jan Meyer
Institute of Electrical Power Systems and High Voltage Engineering
Technische Universität Dresden
Dresden, Germany
friedemann.moeller@tu-dresden.de, sascha.mueller@tu-dresden.de, jan.meyer@tu-dresden.de

***Abstract*— Due to international agreements on climate conferences, Germany has decided to reduce its carbon dioxide emissions. As part of the agenda to achieve that objective, the number of electric vehicles is expected to increase significantly. Electric vehicles (EV) with an on-board charger are mostly single-phase devices utilizing a rectifier with active power factor correction, which usually operate at switching frequencies between 10 and 100 kHz. The single-phase connection can cause unbalance, the power electronics of the rectifier can result distortion below 2 kHz (harmonics) and between 2 kHz and 150 kHz (supraharmonics). In order to ensure Electromagnetic Compatibility, it is important that the emission does not exceed respective limits. The aim of this paper is to analyze the impact of charging infrastructures with high density of EVs on the aforementioned Power Quality phenomena. Therefore the results of three field measurements in central charging infrastructures are presented.**

Electric Vehicles, Power Quality, Unbalance, Harmonics

I. INTRODUCTION

Due to financial incentives in Germany, Electric Vehicles (EV) became profitable for some companies. This has led to an increase of central charging infrastructures (CCI), where a large number of charging points is connected to the same supply point. The parallel charging of multiple vehicles can have a significant impact on Power Quality. Within the framework of the research project "ElmoNetQ" [1], some field studies in CCIs were performed in order to study the summation of network disturbances of multiple EVs and its impact on power quality in public low voltage (LV) networks. This paper discusses the results of these studies considering the impact on unbalance, harmonics and supraharmonics. The emission of the individual electric vehicles, their summation and the total emission of the whole charging facilities are discussed in detail. Unbalance and harmonics propagate in the low voltage grid and can affect the voltage quality in the network. In contrast, supraharmonics majorly stay within the installation and can affect other close-by connected equipment as well as other electric vehicles. Finally, some recommendations for planning and operation of CCIs with respect to a minimized impact on power quality are provided.

This work was supported by the German Federal Ministry for the Environment, Nature Conservation, Building and Nuclear Safety (project ElmoNetQ, FKZ: 16EM1052).

II. MEASUREMENT FRAMEWORK

To study the impact of EV charging on power quality three different CCIs were measured. Supraharmonics has only been measured in the third infrastructure and consequently all three infrastructures are only analyzed with respect to unbalance and harmonics.

A. Grid details

Figure 1 shows a general schematic diagram which applies to all measured sites. A CCI consists of *n* charging boxes (CB), which are connected to a central busbar. This busbar is usually connected via a dedicated feeder (cable) to the LV busbar of the MV/LV substation. Usually no other loads or power plants are connected between these two busbars. At all three sites further feeders, which are supplying different loads like office buildings, public lighting or households, are connected to the LV busbar. The main parameters of the sites are listed in Table I.

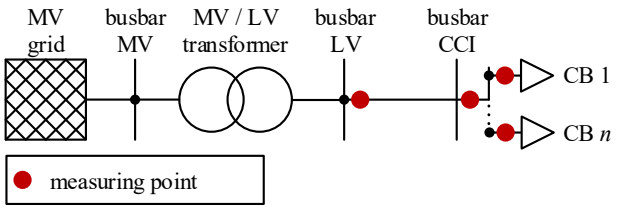

Figure 1. Single line diagram of the network

TABLE I. SITE CHARACTERISTICS

	Site A	Site B	Site C
Short circuit power S_{sc}	4.82 MVA	1.25 MVA	8.89 MVA
Installed power S_A	244 kVA	50 kVA	177 kVA
Maximum utilization S_{ACT}	≈18.4 kVA	≈50 kVA	≈133 kVA
Number and type of charging points	6x type 1 10x type 2	22x type 1	8x type 2

Site A is equipped with 16 charging points: 6 with type-1 socket and 10 with type-2 socket (see Fig. 2). The infrastructure has been specifically designed for a car pool of a company. During the measurement period (one week) only

a few EVs, not representative for the intended utilization, were available. Most of the EVs had a single-phase on-board charger.

Site B is equipped with type-1 sockets for single-phase charging. The CBs are distributed to the three phases of the grid. To avoid a high peak load the number of simultaneously charging EVs is limited by a time shift regime.

Site C was equipped with 8 type-2 sockets and all charged EVs had a three-phase on-board charger.

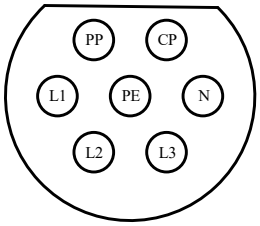

Figure 2. Schema of type-2 socket

B. Measurement details

For all measurements, PQ instruments complying with the requirements of IEC 61000-4-30 class A [2] were used and one-minute averaging interval was selected. Voltage and current magnitudes and phase angles were recorded up to the 50th harmonic. For supraharmonics transient recorders with a sampling rate of 1 MS were used. The measuring time is different between the three sites and varies between six hours and four weeks.

As shown in Fig. 1, the emission of the whole infrastructure and at least of one EV was measured. Depending on the space in the junction boxes and transformer stations, further CBs as well as other loads and feeders were also measured. In this paper only measurements directly related to the EVs are presented.

III. UNBALANCE

This section discusses the impact of EVs on negative-sequence voltage unbalance (k_{u2}), also known as voltage unbalance factor (VUF) [3]. It can be expected that the unbalance is rather low as CCIs provide higher potential to influence the distribution to the phases during planning and operation. The negative-sequence voltage unbalance is defined as

$$k_{u2} = \frac{|\underline{U}_2|}{|\underline{U}_1|} \tag{1}$$

The limit for public low voltage networks is 2 %, according to IEC 61000-2-2 [4]. It should be noted that this value does not correspond to the permissible emission of the charging infrastructure, which is usually much smaller.

To describe the unbalance of the charging infrastructure an unbalanced power is introduced. It can be calculated by using the complex power per phase

$$S_{un2} = \left|\underline{S}_{L1} + \underline{a}^2 \cdot \underline{S}_{L2} + \underline{a} \cdot \underline{S}_{L3}\right| \quad \text{with} \quad \underline{a} = -\frac{1}{2} + j \cdot \frac{\sqrt{3}}{2} \tag{2}$$

Voltage unbalance and unbalance power can be estimated based on the short circuit power at the connection point (S_{sc}) as described in [5]

$$k_{u2} \approx \frac{S_{un2}}{S_{sc}} \tag{3}$$

Another parameter used in this paper is the total power of all three phases

$$S_{total} = S_{L1} + S_{L2} + S_{L3} \tag{4}$$

As limits for unbalance emission of customer installations are currently under revision, an informative maximum unbalanced power can be derived from the limit provided in [6]

$$S_{un2} \leq 0.007 \cdot S_{sc} \tag{5}$$

A. Site A

The type-2 sockets at this site allow all different possibilities of AC-charging including single-phase and three phase charging. Figure 2 shows the schema of this socket type. In case of EVs with a single-phase on-board charger, only L1 and N are usually used for charging. PP and CP are used for communication between EV and CB. Because of the low number of available EVs, only a maximum of five EVs were charged at the same time.

Figure 3 presents the results for unbalance power and voltage unbalance at the busbar of the CCI. The unbalance power is as high as the total power of all three phases, which means that all EVs charge single-phase and use the same phase (L1) for charging. There is also a direct link between total power and voltage unbalance. However, the absolute value of voltage unbalance is low due to the high short circuit power at the connection point and the low number of five simultaneously charging EVs (S_{total} = 18 kVA, which is less than 10 % of the installed power). According to (5) a maximum unbalanced power of 33.7 kVA would be acceptable for this charging infrastructure, which corresponds to about nine single-phase charging EVs connected to the same phase. Consequently if all 16 EVs would be connected in similar way, the unbalance would exceed the permissible limit. Reason for the unfavorable high unbalance contribution is that all EVs use the same connection pin (L1) of the CB (see Fig. 2) and during the construction al sockets of the CBs has been connected in the same way to the grid (similar assignment of phase conductors to the socket pins). To avoid this problem it is recommended to shift the phase allocation of the individual CBs in CCIs.

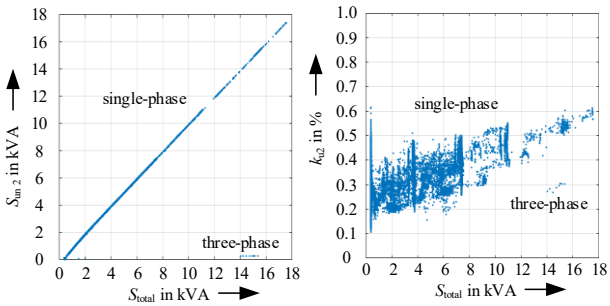

Figure 3. Unbalance power and voltage unbalance depending on the total charging power of site A

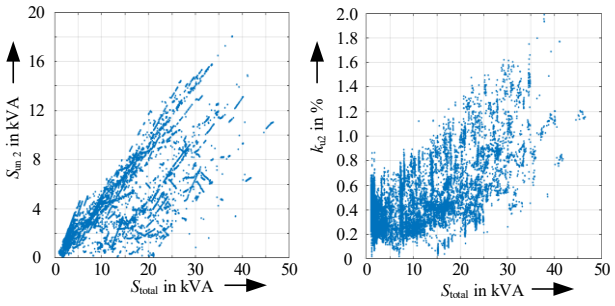

Figure 4. Unbalance power and voltage unbalance depending on the total charging power of site B

B. Site B

In contrast to site A, at site B all CBs (sockets) have been equally distributed to the phases by means of shifting the connection order of the socket pins to the phases of the connection cable. Moreover, an energy management system is used to limit the number of simultaneously charging EVs in order not to exceed the installed power S_A (cf. Tab. I). The balanced distribution of the EVs to the three phases is not included into the management regime. Therefore, even if the energy consumption per phase over a longer time is sufficiently balanced, high unbalances between the phases are still possible.

Figure 4 shows the unbalance power and voltage unbalance depending on the total power. Even though the total power can reach up to 100 % of the installed power $S_A = 50$ kVA (about 14 simultaneously charging EVs), the unbalance power is not higher than 18 kVA, which corresponds to 5 EVs. This proves that even a perfect distribution of the CBs to the phases of the network does not ensure perfectly balanced loading due to the customer behavior. Similar results have been also obtained for distributed infrastructures [7]. Due to the lower short circuit power the maximum permissible unbalance power for this charging infrastructure is only 8.75 kVA, which corresponds to 2 till 3 EVs. The maximum measured voltage unbalance amounts almost 2 % (limit according to [4]). This confirms that the contribution of this charging infrastructure to the unbalance voltage is with an unbalanced power of 18 kVA already too high and should be reduced.

The results show that even in case of a CCI with CBs equally distributed to the phases of the grid, high unbalance levels are possible. Besides using three-phase-chargers it is recommended to include unbalance as additional parameter into charging management systems.

C. Site C

At site C only EVs with true three-phase chargers are used. Consequently even at a total power $S_{total} = 120$ kVA (71 % of installed power), which is more than two times the total power at site B, the unbalance power did never exceed $S_{un2} = 0.5$ kVA. The unbalance power was mainly caused by the power consumption of the power electronics of the CBs. According to (5) a maximum unbalance power of 62 kVA would be permissible due to the very high short circuit power. The CCI has no negative affect on the voltage unbalance. This underlines that the most efficient way of charging in terms of network utilization is always three-phase charging and whenever possible three-phase chargers should be used.

IV. HARMONICS

Harmonics are a part of the low-frequency emission in the range up to 2.5 kHz. Harmonic voltage limits in public LV grids are defined in the standard IEC 61000-2-2 [4]. In order to comply with those limits and to avoid negative impacts on other connected devices, the current emission of large installations such as CCIs has to meet the requirements as defined in [6] and which are calculated according to the following equation:

$$I^{(h)} = \frac{p_h}{1000} \cdot \sqrt{\frac{S_{sc}}{S_A}} \cdot I_A \qquad (7)$$

Beside the ratio of the short circuit power of the grid at the PCC S_{sc} and the total installed power of the infrastructure S_A, proportionality factors p_v for the individual harmonic orders are required (Tab. II). The absolute emission limits depend on the total current of the installation I_A.

TABLE II. PROPORTIONALITY FACTORS P_H (PHASE CURRENTS)

v	**3**	**5**	**7**	**11**	**13**
p_v	6	15	10	5	4

It should be noted that the emission limit assessment according to [6] is specified for the 95th percentile of the 10-minute values over one week. As measurement time and averaging interval for each measurement has been slightly different, the results should be treated as an indication.

A. Site A

The 99th percentile of the harmonic currents is presented in Fig. 5a. As only less than 10 % of the installed power has been utilized during the measurements (5 EVs in one phase), most of the currents are relatively small with the highest magnitude at the 5th harmonic with around 2.5 A. The

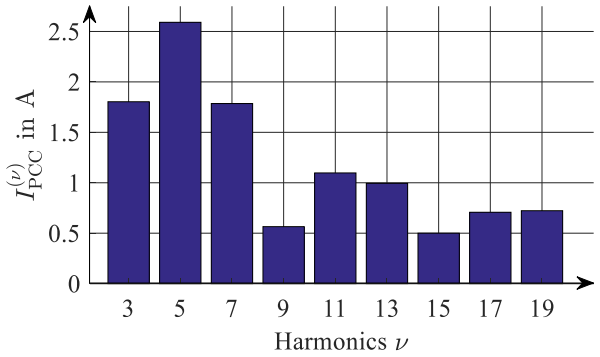

(a) 99th percentile of the harmonic currents during the charging of EVs

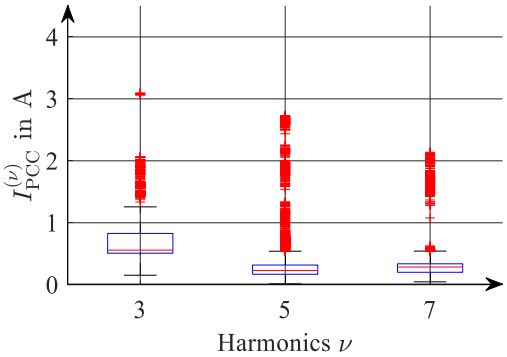

(b) Distribution of the harmonic currents during the measurement

Figure 5. Harmonic currrents at site A

percentage share of different numbers of simultaneously charging EVs over the time is given in Tab. III. However, only the time, in which at least one EV was connected, is considered. The percentage share of three or more simultaneously connected EVs is again only at around 10 %.

TABLE III. PERCENTAGE SHARE OF SIMULTANEOUSLY CHARGING EVS

Number of EVs	**1**	**2**	**3**	**4**	**5**
Share in %	60.97	29.04	8.89	0.81	0.29

As an example, the distribution of the three most significant harmonic currents (3rd, 5th, 7th) is shown in Fig. 5b. Most of the time the harmonic currents are very low as the number of EVs is less than three. However, it should be noted that the variation of the harmonic currents is not only caused by the number of EVs but also by the type of EVs and by the background voltage distortion. Further details on this issue can be found in [8].

The emission limits (cf. Tab. IV) for the CCI are significantly higher than the measured values, which correspond to the 99th percentile magnitude (cf. Fig. 5a). While the CCI is utilized only by about 8 %, the emission is already between 10 % and 20 % of the respective limits. However, a linear extrapolation for this site is most likely too conservative as different types of EVs with different emission characteristic are connected and consequently, a certain harmonic cancellation can be expected [9].

TABLE IV. ASSESSMENT OF EMISSION LIMITS ($S_{ACT}/S_A \approx 8$ %)

Harm. order	3	5	7	11	13
I_{lim} (A)	9.4	23.5	15.7	7.8	6.3
I_{meas} (A)	1.8	2.6	1.8	1.1	1.0
I_{meas}/I_{lim} (%)	19.2	11.0	11.4	14.0	15.9

B. Site B

At site B a maximum of 14 EVs has been charged simultaneously. The single-phase charging EVs were distributed equally to the phases. Fig. 6a presents the 99th percentile values of the harmonic magnitudes. Compared with the respective spectrum of site A (cf. Fig. 5a), the 3rd harmonic current shows higher values. However, the magnitudes decrease strongly with the harmonic order. The distribution of the major harmonic current magnitudes (3rd, 5th and 7th harmonic) over the time is shown in Fig. 6b. If the EVs are more or less equally distributed to the three phases, the harmonics with zero sequence characteristic, like the 3rd harmonic, add up nearly arithmetically in the neutral conductor. Consequently, the neutral conductor loading is

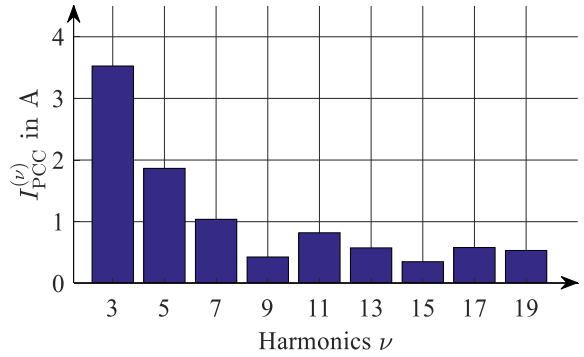

(a) 99th percentile of the harmonic currents during the charging of EVs

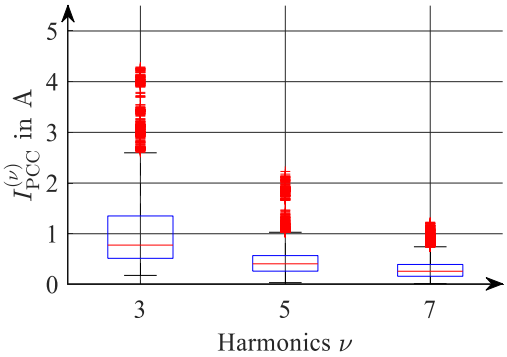

(b) Distribution of the harmonic currents during the measurement

Figure 6. Harmonic currrents at site B

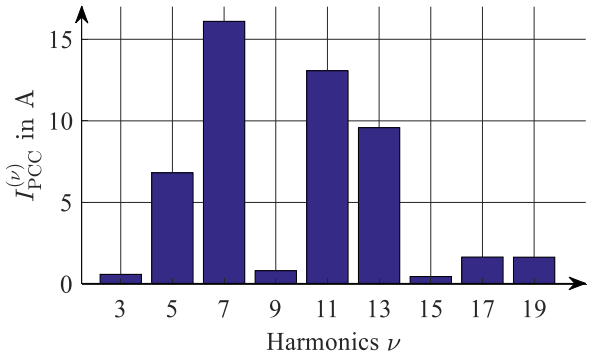

(a) 99th percentile of the harmonic currents during the charging of EVs

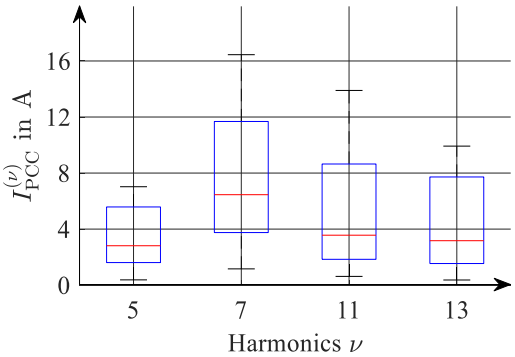

(b) Distribution of the harmonic currents during the measurement

Figure 7. Harmonic currrents at site C

about three times the value presented in Fig. 6.

The assessment of emission limits is presented in Table V. In contrast to site A, the CCI is utilized by about 100 % and the measured values can be directly compared to the limits. While the 3rd harmonic current exceeds the limit, the values of all other considered harmonics are with more than 50 % below the limits.

TABLE V. ASSESSMENT OF EMISSION LIMITS ($S_{ACT}/S_A \approx 100$ %)

Harm. order	3	5	7	11	13
I_{lim} (A)	2.2	5.4	3.6	1.8	1.4
I_{meas} (A)	3.5	1.9	1.0	0.8	0.6
I_{meas}/I_{lim} (%)	162.9	34.5	28.8	45.5	39.8

C. Site C

During the measurement at site C a maximum of six EVs (three-phase charger) of the same type have been connected consecutively to the grid. In the harmonic current spectrum (cf. Fig. 7a) the magnitudes of the 5th, 7th, 11th and 13th order are dominating, whereas the zero-sequence harmonics (as e.g. 3rd, 9th and 15th harmonic) are very small due to the three-phase topology of the EV charger. With a magnitude of around 16 A the highest value occurred for the 7th harmonic. Similar to the other sites, Fig. 7b shows the variation range of the 5th, 7th, 11th and 13th harmonic current. Due to the fact, that the EVs are from the same type, their harmonic currents virtually add up arithmetically [9].

When applying the rules defined in [6], the emission limits as shown in Tab. VI are obtained. It is obvious, that for the 11th and 13th order the limits are violated significantly, even though the utilization of the CCI was only at 75 %. Therefore, the connection of larger numbers of EVs of this type has to be considered carefully and mitigation measures might be required.

TABLE VI. ASSESSMENT OF EMISSION LIMITS ($S_{ACT}/S_A \approx 75$ %)

Harm. order	3	5	7	11	13
I_{lim} (A)	10.9	27.2	18.1	9.1	7.2
I_{meas} (A)	0.6	6.8	16.1	13.1	9.6
I_{meas}/I_{lim} (%)	5.5	25.1	88.9	144.4	132.3

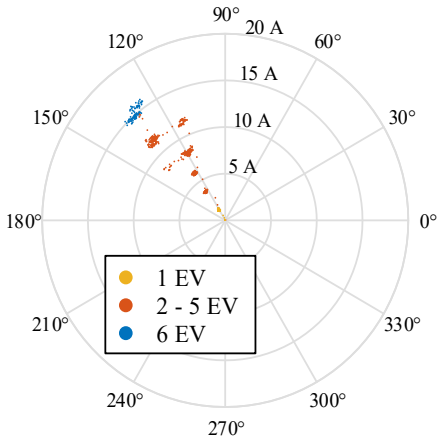

(a) 7th harmonic current

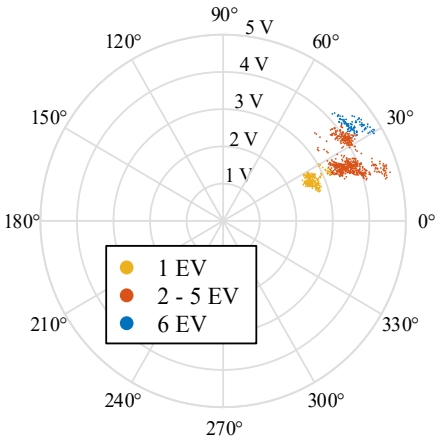

(b) 7th harmonic voltage

Figure 8. 7th harmonic current and voltage during the sequential connection of six EVs

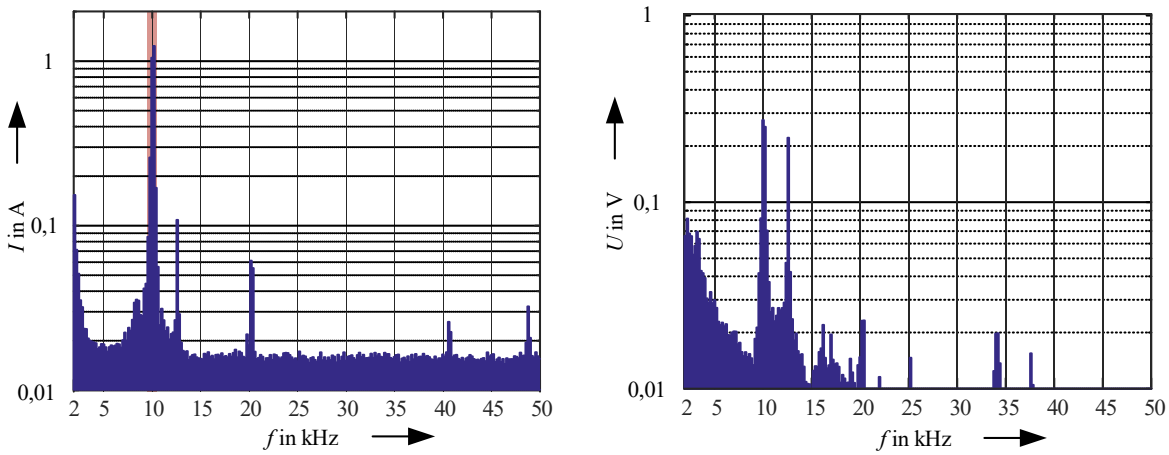

Figure 9. Supraharmonics current and voltage when a single EV is connected

Because of the very high magnitude of the 7th harmonic current, its behavior during the sequential connection of the EVs is studied in more detail. The respective polar plots of both the current and the voltage are shown in Fig. 8. The plots exhibit a very significant increase of the magnitudes, while the respective phase angles show only a very small variation. This means that the 7th current harmonic of the EVs adds up almost arithmetically (no primary cancellation). With respect to the 7th voltage harmonic this indicates that the voltage drop over the network impedance caused by the 7th harmonic current of the EVs adds up nearly arithmetically with the respective background harmonic voltage (no secondary cancellation). The small shift of the phase angle, which is still visible, can be explained by a slight change of the background voltage during the measurement. Further details on cancellation can be found in [10]. An example of an effective cancellation between EVs and a heat pump can be found in [11]. In contrast to the other sites and despite the high short circuit power of the grid at the connection point, the effect of the current distortion on the voltage distortion is remarkable and cannot be neglected.

V. SUPRAHARMONICS

Supraharmonics describe the emission in the frequency range between 2 kHz and 150 kHz. EV chargers, namely the active PFC of the rectifier, are a significant source of such emission [12]. The analysis for this paper is based on a method provided in IEC 61000-4-7 [13] for the frequency range 2-9 kHz. The measurement signal is highpass-filtered and divided into gapless 200-ms-windows. The application of a DFT results in a spectrum with a frequency resolution of 5 Hz for each measurement window, which is aggregated in frequency into 200-Hz-bands with the center frequency b:

$$Y_{\mathrm{SH,b}} = \sqrt{\sum_{f=b-95}^{b+100} Y_{C,f}^2} \qquad (8)$$

The symbol Y in (8) can represent either voltage or current.

The supraharmonic emission of EVs is analyzed for site C only, as no supraharmonic measurements have been performed at sites A and B. All EVs at site C are from the same type and have a three-phase on-board charger. Like in the last part of section IV.C also the stepwise connection of six EVs is analyzed. Table VII gives an overview of the connection order.

TABLE VII. CONNECTION ORDER OF EVS TO THE CHARGING BOXES

EV	1	2	3	4	5	6
CB	1a	2a	4a	3a	1b	4b

Results are presented and discussed for one phase as the results for the other phases are similar. Figure 9 shows supraharmonic currents and voltages in the frequency range between 2 and 50 kHz when only one EV (EV 1) is charging. Frequencies above 50 kHz are not presented, because no significant magnitudes has been observed. The emission around 10 kHz is caused by the switching frequency of the active PFC of the EV itself and is also referred to as primary emission. The frequencies around 20 kHz and 40 kHz

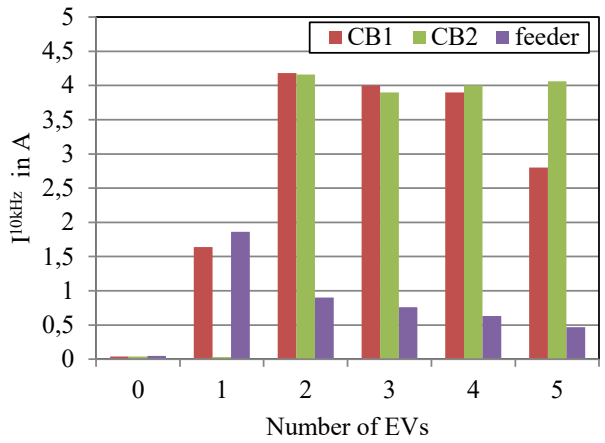

Figure 10. Supraharmonic current emission of the first emission band around EV swiching frequency depending on the number of EVs

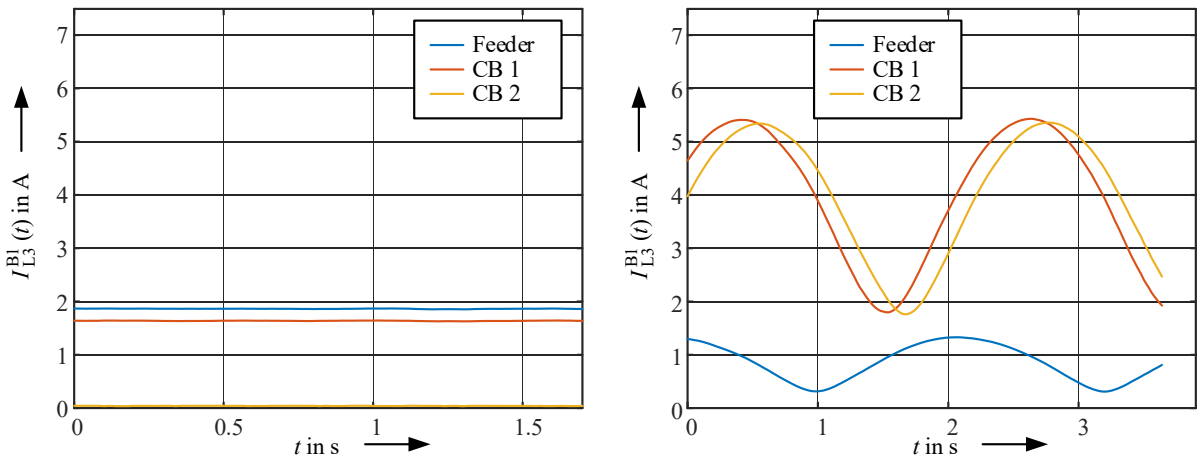

Figure 11. Supraharmonic current emission of the first emission band around EV swiching frequency for one (left) and two (right) connected EVs

correspond to the 2nd and 4th harmonic of the switching frequency. The frequency component around 12.6 kHz is emitted by another device in the grid. The current flowing into the EV charger is determined by the input impedance of the EV charger at this frequency (sink characteristic). This part of the emission is also referred to as secondary emission. Further details on the concept of primary and secondary emission can be found in [14]. As the input impedance of equipment in the supraharmonic range can become rather low, significant interactions between the equipment can be expected.

In order to study this interaction as well as the summation characteristic in more detail, the emission levels around the switching frequency of the EV depending on the number of charging cars are analyzed. Even if the EVs are all of the same type, the switching frequencies will slightly vary between them, e.g. due to manufacturing tolerances. To cover most of the energy emitted at switching frequency (first emission band B1), the bandwidth of the analyzed frequency band is extended to 1 kHz and centered around the switching frequency of 10 kHz (see red band in Fig. 9):

$$I^{B1} = \sqrt{\sum_{f=9500\,\mathrm{Hz}}^{10500\,\mathrm{Hz}} I_{C,f}^2} \qquad (7)$$

The results are presented in Fig. 10. When the first EV is connected to CB1, as expected the feeder current flowing into the grid is almost similar to the current of the charging box (about 1.7 A). The higher value compared to Fig. 9 results from the five times larger frequency bandwidth. Connecting the second EV to CB2 changes the situation completely. Now a very high current of about 4 A is flowing between the two EVs while the feeder current reduces to less than 1 A. This significant change can be explained by the change of the impedance situation. The grid side impedance at 10 kHz is significantly higher than the input impedance of the EVs. As the EV charger acts more like a voltage source the reduction of impedance due to the connection of the second EV increases the current considerably, which flows mainly along the low impedance paths through the EVs. Connecting more EVs reduces the feeder current even more (cf. Fig. 10), and most of the emission stays within the charging infrastructure. This behavior is typical for supraharmonic emission.

While Fig. 10 presents an average value of about 3-second-intervals, Fig. 11 shows the time characteristic of the switching frequency emission based on measurement windows of 20 ms (about 1 cycle at power frequency). According to Fig. 11 left the time characteristic of the current of the first emission band for one connected EV is constant. If two EVs are connected (Fig. 11 right), a significant beating can be observed both in the currents of the charging boxes as well as the feeder current flowing into the grid. The beating is caused by the slightly different switching frequencies of two EVs. The beating frequency corresponds to the half of the difference of the switching frequencies, which is about 1 Hz for these two EVs.

Other measurements have shown that the high supraharmonic current of one EV can cause an interruption of the charging process of another EV connected to the same charging box. To avoid this, it is recommended to increase the immunity of devices on supraharmonics and the input impedance of the EVs for higher frequencies.

VI. Recommendations

Recommendations to minimize the network disturbances of EV charging are divided into two parts. The first part relates to planning and operation of new CCIs, while the second part addresses the standardization and the manufacturers of EVs.

A. Planning of Central Charging Infrastructures

Presently, many EV types are equipped with a single-phase on-board charger with a plug for type-2 sockets, where the charging rectifier is connected to pin L1. To avoid a high unbalance it is recommended to distribute the “L1”-pin of the type-2 socket in the CBs (see Fig. 2) as well as the phase conductors of type-1 sockets (single-phase) CBs equal to the phase conductors of the grid. If charging management systems are installed, it is recommended to include not only total charging power but also the unbalance into the

management regime of the CCI. This can be implemented in different ways, like: charge the same number of EVs per phase, connect new EVs to the phase conductor with the lowest current or by reduction of the charging current per EV and phase depending on the number of simultaneously charging EVs.

Another option to reduce the impact on network disturbances, especially on unbalance and harmonics, is an increase of short circuit power at the busbar of the CCI e.g. by using a separate feeder, parallel cables and/or a dedicated MV/LV transformer.

B. Standardization and EV Manufacturers

The best method to reduce the impact of EV charging on unbalance is the use of three-phase on-board chargers. If symmetrical three-phase charging is not possible, the charging power should not exceed 3.7 kVA per phase. Charging with two single-phase chargers on different phases is better compared to charging between two phases.

With respect to harmonics, future standardization work should account for the voltage-dependent current emission of EVs (e.g. in [15]). By implementing additional requirements, the robustness of EVs with respect to supply voltage distortion should be improved. One option is to limit the difference in emission between sinusoidal test voltage and a set of distorted test voltages. The specification of a frequency-dependent input impedance characteristic improves also the robustness of the charger and can helps to avoid possible network resonances.

To avoid interferences caused by supraharmonics between EVs as well as EVs and other devices, emission limits for supraharmonic emission are urgently required. At present limits exist only for frequencies up to 2 kHz and higher than 150 kHz [16]. It is further recommended to consider the effect of beating (Fig. 11) as well as the specification of an impedance characteristics like already proposed for harmonics.

VII. CONCLUSION

Field studies of three different central charging infrastructures (CCIs) show that EVs can have considerable and adverse impact on unbalance, harmonics and supraharmonics. In order to ensure acceptable levels for the mentioned network disturbances they should be consider in the planning stage for new CCIs. Some effects can already be efficiently reduced by careful planning. In case a charging management system is implemented, it should be considered to include also power quality into the management regime. Finally several gaps in standardization, especially with respect to the frequency range 2 to 150 kHz have to be closed as fast as possible. Joint effort of network operators and EV manufacturers is required to ensure EMC, especially if larger CCIs are realized in the future.

At present the authors work on simplified guidelines to estimate the maximum allowable number of EVs for CCIs with respect to power quality and suggestions, how the number can be cost-effectively increased.

ACKNOWLEDGMENT

The authors gratefully acknowledge the support of the measurements by DREWAG Netz GmbH, ED Netze GmbH and Deutsche Post AG.

REFERENCES

[1] TU Dresden/IEEH: Abschlussbericht zum Porjekt ElmoNetQ: “ Auswirkungen einer zunehmenden Durchdringung von Elektrofahrzeugen auf die Elektroenergiequalität in öffentlichen Niederspannungsnetzen“, Bundesministerium für Umwelt, Naturschutz, Bau und Reaktorsicherheit (BMUB), 2017

[2] IEC 61000-4-30:2015 Electromagnetic compatibility (EMC) – Part 4-30: Testing and measurement techniques – Power quality measurement methods

[3] A. von Jouanne, B Banerjee, “Assessment of Voltage Unbalance”, IEEE Transactions on Power Delivery, Vol. 16, No. 4, pp. 782-790, October 2001

[4] IEC 61000-2-2:2002 Electromagnetic compatibility (EMC) – Part 2-2: Environment – Compatibility levels for low-frequency conducted disturbances and signalling in public low-voltage power supply systems

[5] A. B. Baggini, “Handbook of power quality”, Chichester, England: John Wiley & Sons, 2008

[6] DACHCZ: Technische Regeln zur Beurteilung von Netzrückwirkungen, 2nd Edition, 2007

[7] F. Möller, S. Müller, J. Meyer, P. Schegner, C. Wald, S. Isensee, “Impact of Electric Vehicle Charging on Unbalance and Horminc Distortion – Field Study in an Urban Residential Area“, 23rd International Conference on Electricity Distribution (CIRED), Lyon, 2015

[8] S. Müller, J. Meyer, P. Schegner, S. Djokic, "Harmonic Modeling of Electric Vehicle Chargers in Frequency Domain," International Conference on Renewable Energies and Power Quality (ICREPQ), La Coruña, 2015

[9] J. Meyer, S. Müller, S. Ungethüm, X. Xiao, A. Collin, S. Djokic, "Harmonic and Supraharmonic Emission of On-Board Electric Vehicle Chargers," IEEE PES Transmission and Distribution Conference and Exposition-Latin America (T&D LA), Morelia, 2016

[10] J. Meyer, A. M. Blanco, M. Domagk, P. Schegner, "Assessment of Prevailing Harmonic Current Emission in Public Low Voltage Networks," IEEE Transactions on Power Delivery, Vol. 32, No. 2, pp. 962-970, April 2017

[11] A. A. Malano, S. Müller, J. Meyer, S. Bachmann, "Harmonic Interaction of Electric Vehicle Chargers in a Central Charging Infrastructure," 17th International Conference on Harmonics and Quality of Power (ICHQP), Belo Horizonte, 2016

[12] S. Schöttke, J. Meyer, P. Schegner, S. Bachmann: “Emission in the Frequency Range of 2 kHz to 150 kHz caused by electrical vehicle charging”, IEEE International Symposium on Electromagnetic Compatibility (EMC Europe), Gothenburg, 2014

[13] IEC 61000-4-7:2002 Electromagnetic compatibility (EMC) – Part 4-7: Testing and measurement techniques – General guide on harmonics and interharmonics measurements and instrumentation, for power supply systems and equipment connected thereto

[14] M. H. J. Bollen and S. K. Rönnberg, "Primary and secondary harmonics emission; harmonic interaction - a set of definitions," 17th International Conference on Harmonics and Quality of Power (ICHQP), Belo Horizonte, 2016

[15] IEC 61000-3-2:2014 Electromagnetic compatibility (EMC) – Part 3-2: Limits – Limits for harmonic current emission (equipment input current ≤ 16 A per phase)

[16] IEC 61851-21-1/Ed. 1: Electric vehicle conductive charging systems - Part 21-1: Electric vehicle onboard charger EMC requirements for conductive connection to an a.c./d.c. supply